Chapter VI

Synthesis and Characterization of Core-Shell Nanoparticles

Core-Shell nanoparticles are hybrid systems. They have a core and a shell having distinct attributes such as metallicity, semiconductivity, magnetism etc. These systems are fascinating as they can protect the core from the chemical environment of the medium. The ability to synthesize semiconductor nanocrystals with narrow size distribution and high luminescent efficiencies in core-shell model has enhanced their application in opto-electronic devices.

Most studies have shown that the surface of the nanocrystals plays a major role in their physical properties and especially in the recombination processes of the excited carriers. The surface is indeed composed of a large number of dangling bond and defects, and these nanoparticles have a large surface to volume ratio.

The best way to improve the quality of the particles is to achieve chemical passivation of the surface of the crystallites in order to eliminate any traps for electrons and holes. This can be successfully achieved by having an inorganic coating of the semiconductor nanoparticles to produce some kind of core/shell nanostructures. The basic idea is to cover the nanoparticle with another semiconductor, the band gap position of which allows the confinement of the electron and holes inside the inner core particle. Since the two compounds have a close crystal structures, epitaxial growth of the shell semiconductor onto the core may occur and should ensure that no defects act like traps in the interface. This chapter focuses on the synthesis and characterization of mixed CdS–ZnS core-shell nanoparticles in organic phase.

6.1 Introduction

Since the beginning of the 1980s, the field of low dimensional systems has been extensively investigated. Semiconductor nanocrystalline constitute an intermediate state between a molecule and a bulk material. When a crystal size is reduced to the size of exciton Bohr radius, drastic changes in physical properties are found as a consequence of quantum confinement effects. For fundamental and technological applications, new developments are strongly dependent on the ability to have control over the production of crystallites with well defined structural properties such as chemical composition, crystallography, mean size, morphology and surface [1]. For spherical semiconductor nanocrystals, a proven strategy for increasing both the fluorescence quantum yield and the stability is to grow a shell of a higher band gap semiconductor on the core nanocrystal [2-4]. If the band offsets between the core and the shell materials are such that the band gap of the core is enclosed by that of the shell, in a configuration known as type I, then the electron and hole wave functions may be confined to the core region, reducing the probability for non radiative decay via surface states and traps [5]. The ability to synthesise semiconductor nanocrystals with narrow size distribution and high luminescent efficiencies has made QDs an attractive alternative to organic molecules in applications such as opto-electronic devices [6,7] and biological fluorescence labelling [8-10].

The size tunable optical properties of quantum dots are independent of their chemical properties, along with their stability and saturated colour emission have made them particularly interesting as the active materials in large area (cm^2) hybrid organic / inorganic QD light emitting devices (QD-LEDs) [11-13].

Several synthetic routes such as chemical precipitation, sol-gel, microemulsion and inverse miscelles have been used to grow core-shell chalcogenides nanoparticles with an emphasis on better control over size, shape and size distribution.

The controlled growth of nanoparticles in supporting matrices such as, glasses, [14] zeolites [15] and polymers with tuneable optical properties has been investigated. Langmuir-Blodgett (LB) technique has been used for preparing quantum size nanoparticles of sulphides and selenides [16]. The presence of layered structure and molecular order in LB films is expected to assist in achieving better control over size, shape and size distribution of nanoparticles.

The most common solution based methods for nanoparticles synthesis with precise control of size and shape are organometallic [17] and water–in–oil micro-emulsion routes [18]. In the organo-metallic method, organic metal precursors are heated at high temperatures (250˚ – 300˚C) in a coordinating solvent, leading to a reaction of precursors, nucleation and growth of nanoparticles. This method has been extensively used for the synthesis of II-VI and III-V semiconductors [19] and metals also. Size-control is achieved by varying reaction temperature, initial precursor concentration and by further intermediate injection of precursors, if necessary.

Water-in-oil microemulsions are self assembled surfactant templates of nanometer size, which can be spherical, cylindrical or of other desired shape dispersed in a continuous oil medium. Water with a predissolved reactant added into the microemulsion solution goes inside the templates and there by forms nanometer-sized spherical water droplets, acting as size and shape controlled nanoreactors [18]. Appropriate reactants in the water drops of two different microemulsions are mixed together for nanoparticles synthesis by reactive precipitation. The drops collide

because of Brownian motion, coalesce and exchange their contents thus bringing the two reactants together inside a single drop for reaction.

6.2 Experimental Details

Chemicals:

All chemicals used were of analytical grade and were used as received without further purification.

$Cd(NO_3)_2$ - Cadmium Nitrate

$C_{18}H_{36}O_2$ - Stearic Acid

$CHCl_3$ - Chloroform

$C_{18}H_{38}S$ - Octadecane Thiol

$Zn(NO_3)_2$ - Zinc Nitrate

Sample Preparation:

For synthesis of CdS-ZnS core-shell nanoparticles, initially the procedure for synthesis of CdS nanoparticles in organic phase as described in Chapter 4 is used (Page No. 73 & 74). The CdS nanoparticles so synthesized are mixed with 10^{-3} M aqueous solution of $Zn(NO_3)_2$ whose pH is adjusted to 8.5 by using liquid ammonia. This mixture is stirred using a magnetic stirrer for 5 hours. The Zn ions from the aqueous state are transferred to chloroform organic phase forming a shell over the CdS core. Add equal volumes of 5×10^{-3} M ODT dissolved in chloroform to the mixture. ODT behaves as a capping agent so that the Zinc ions do not agglomerate. The solutions are mixed well by shaking and the mixture is kept aside for 15 minutes. Then H_2S gas is bubbled through the mixture for 15 minutes. The stable CdS core ZnS shell nanoparticles in organic phase are synthesized.

Similarly, for synthesizing ZnS-CdS core-shell nanoparticles, initially the procedure for synthesis of ZnS nanoparticles in organic phase in Chapter 5 is used (Page No.101 & 102). The ZnS nanoparticles so synthesized are mixed with 10^{-3} M aqueous solution of Cd $(NO_3)_2$ whose pH is adjusted to 8.5 using liquid ammonia. This mixture is stirred using a magnetic stirrer for 5 hours. The Cd ions from the aqueous state are phase transferred to organic phase forming a shell over the ZnS core. To equal volumes of phase transferred cadmium, add 5 x 10^{-3} M ODT dissolved in chloroform. ODT behaves as a capping agent so that the cadmium ions do not agglomerate. The solutions are mixed well by shaking and the mixture is kept aside for 15 minutes. Then H_2S gas is bubbled through the mixture for 15 minutes. The ZnS core CdS shell nanoparticles in organic phase are synthesized.

The samples so obtained, CdS/ ZnS core shell and ZnS/ CdS core shell were characterized by different techniques.

6 .3 UV Visible Spectroscopy

Fig. 6.1 shows the UV-vis absorption spectra of the core-shell nanoparticles. Curve 1 shows the absorption spectrum of CdS core ZnS Shell and curve 2 shows the absorption spectrum of ZnS core CdS shell.

The absorption spectra are broad and do not present clear structures owing to quantum confinement. The characteristic excitonic peak centred around 300 nm (E*g* = 4.13eV) in both the core shell structures reveals the quantum confinement effect [1]. The samples showed absorption peak at smaller wavelengths compared to bulk CdS, which shows a peak at 512 nm (E*g*=2.7 eV). This confirms the formation of CdS nanoparticles. The peak positions of core shell spectra are red-shifted compared to their corresponding core CdS nanoparticles. This clearly indicates an increase in the

overall nanoparticle diameter, as a result of growth of the ZnS (E*g* = 3.6 eV of the bulk ZnS) shell around the core particles.

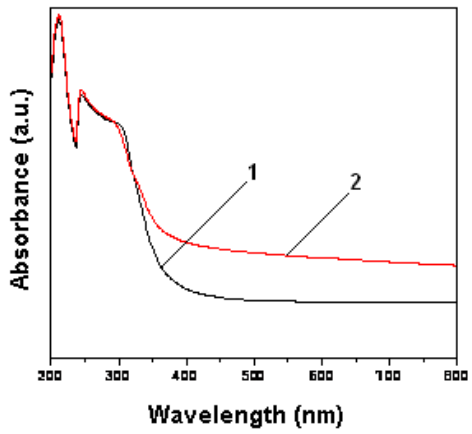

Fig. 6.1 *UV-visible absorption spectrum of ODT capped CdS-ZnS core-shell nanoparticles (1) and ODT capped ZnS-CdS core-shell nanoparticles (2).*

Similarly the absorption spectra of the ZnS core and CdS shell show a broad spectrum. It indicates quantum confinement. The absorption peak occurs at a shorter wavelength compared to bulk ZnS. The peak positions of the core spectrum are red shifted. This accounts for the formation of the CdS shell over ZnS core.

6.4 XRD Measurements

XRD analysis of the drop coated films on silica substrate from ODT – capped CdS core/ ZnS shell nanoparticles and ODT capped ZnS core/ CdS shell nanoparticles was carried out on a Xpert PANalytical instrument operating at 40 *k*V and a current of 30*m*A with Cu *K*α radiations. These patterns have been recorded within the range of 30˚ - 70˚ with a scan rate of 2˚ / min.

Fig. 6.2(A) shows the diffraction patterns of ODT capped CdS core / ZnS shell nanoparticles. They represent crystalline pattern showing the presence of CdS and ZnS. The diffraction patterns of core-shell nanocrystals show a noticeable influence of CdS shell. The standard 2θ values of β-CdS cubic structure are 43.917˚

(220) and 51.911˚ (311) (Ref. Code 00-001-0647). The observed 2θ values are 44.58˚ and 52.15˚. They correspond to the lattice planes of cubic CdS structures. The broadening of the XRD pattern takes place due to nano-crystalline nature of the sample.

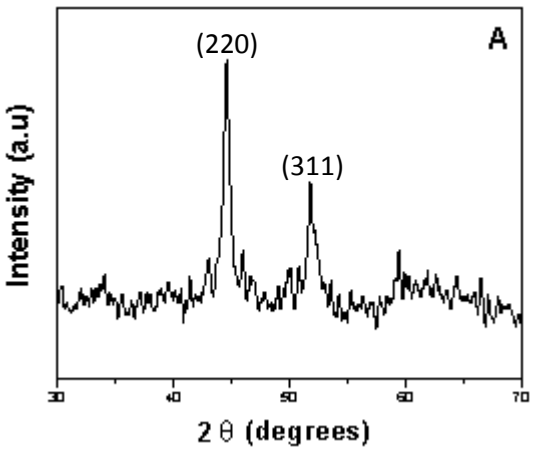

Fig. 6.2(A) *XRD pattern of drop coated film on Si(111) substrate from CdS-ZnS core-shell nanoparticles Bragg reflections are indexed.*

Fig 6.2 (B) shows the diffraction pattern of ODT capped ZnS core/ CdS shell nanoparticles. Thus, the nanocrystalline core-shell model could be synthesized at room temperature in chloroform with ODT capping agent. The strongly oriented (220) growth is attributed to the formation of CdS and ZnS nanoparticles.

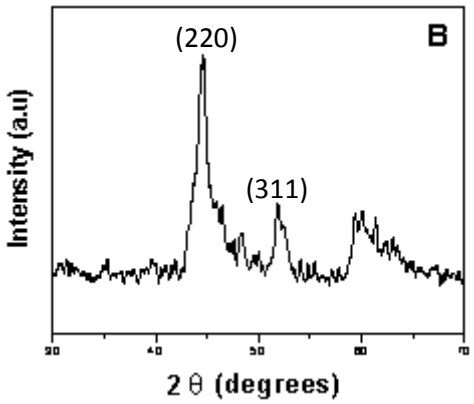

Fig. 6.2(B) *XRD pattern of drop coated film on Si(111) substrate from ZnS-CdS core-shell nanoparticles Bragg reflections are indexed.*

The broadening of the XRD pattern is larger indicating that the sample is nano-crystalline in nature. The observed 2θ values are 44.58˚ and 52.15˚ (same as CdS core / ZnS shell) corresponding to the cubic CdS structure.

6.5 Fourier Transform Infra Red Spectroscopy

FTIR measurements have been made in the wave number range 1000 cm^{-1} and 4000 cm^{-1}

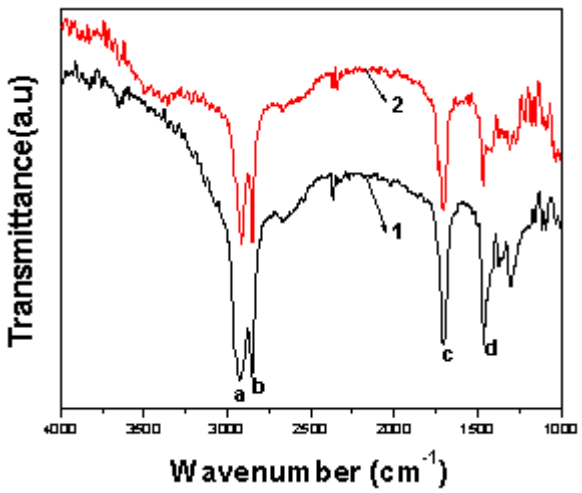

Fig. 6.3 *FTIR spectra recorded from drop coated film on Si(111) Wafer of CdS-ZnS core-shell nanoparticles (1) and ZnS-CdS core-shell nanoparticles (2).*

Fig. 6.3 illustrates the FTIR measurements of cadmium sulphide core and zinc sulphide shell nanoparticles (curve 1) and Zinc sulphide core and cadmium sulphide shell nanoparticles (curve2).

Both the samples show two stretching bands asymmetric and symmetric between 2900 cm^{-1} - 3000 cm^{-1} are assigned to C-H stretching (a and b). Absorption bands near 1750 cm^{-1} is associated to the C – O carboxylic stretch (c). Very weak bending vibration appears at 1600 cm^{-1} due to C – C stretching. Bands around 900 – 1500 cm^{-1} are due to oxygen stretching and bending frequency (d). However, S- H

stretching vibration found in ZnS nanoparticles are not prevalent in the core shell model in the band near 2600 cm $^{-1}$ – 2500 cm $^{-1}$.

6.4 Particle size measurements

The Particle Size Distribution (PSD) of cadmium sulphide core and Zinc Sulphide shell nanoparticles in organic phase is in the range of 100 nm – 200nm size. The particle size distribution of CdS / ZnS core shell nanoparticles are represented in Fig. 6.4 (A). About 70% of the particles have a size of less than 150 nm. Around 30% of the particles have a size of 150 nm - 200nm size.

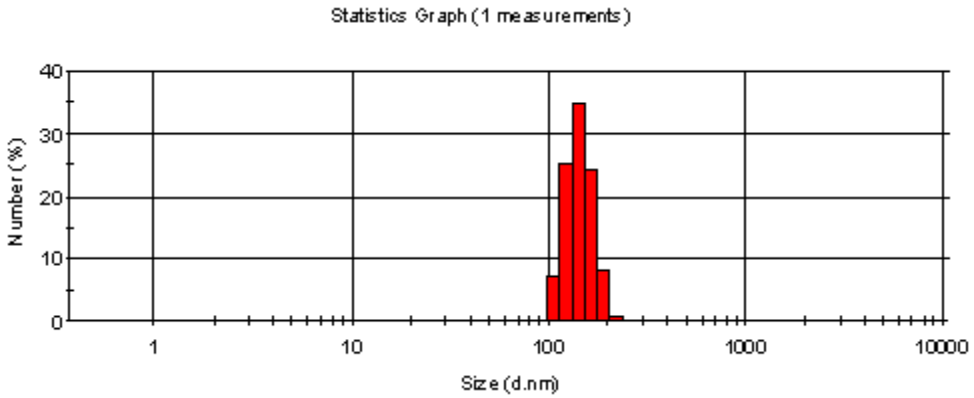

Fig. 6.4 (A) *Histograms showing particle size distribution of CdS-ZnS core-shell nanoparticles.*

Fig. 6.4(B) illustrates the particle size distribution of ZnS core and CdS shell nanoparticles. 45% of the nanoparticles have a size less than 100 nm. They lie in the range of 80 nm – 100 nm. 90% particles have a size less than 120 nm. The particle size distribution is indicative of the quantum confinement of the particles

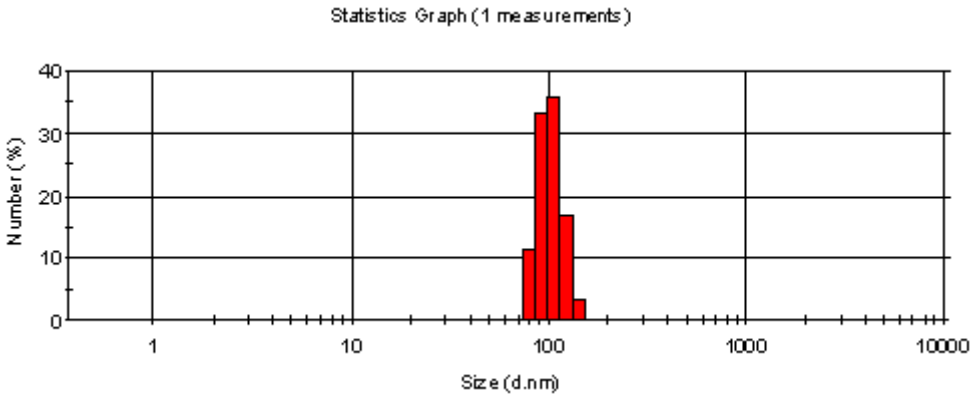

Fig. 6.4(B) *Histograms showing particle size distribution of ZnS-CdS core-shell nanoparticles.*

6.5 Zeta Potential measurements

Zeta potential is one of the main forces that mediate inter- particle interaction. Most particles acquire a surface charge, principally either by ionization of surface group or adsorption of charged species. These surface charges modify the distribution of the surrounding ions, resulting in a layer around the particle that is different to the bulk solution.

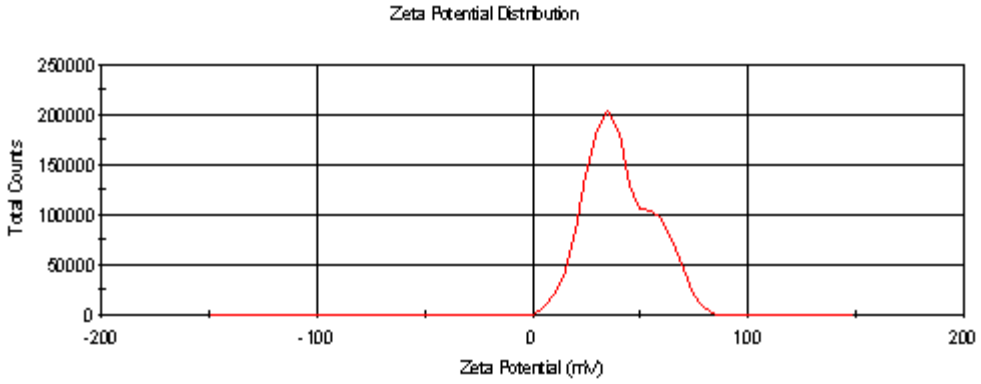

Fig. 6.5(A) *Zeta potential plot of CdS-ZnS core-shell nanoparticles.*

Fig. 6.5(A) illustrates the zeta potential measurements of Cadmium sulphide core and zinc sulphide shell nanoparticles. Fig. 6.5(B) shows the zeta potential measurements of zinc sulphide core and cadmium sulphide shell nanoparticles.

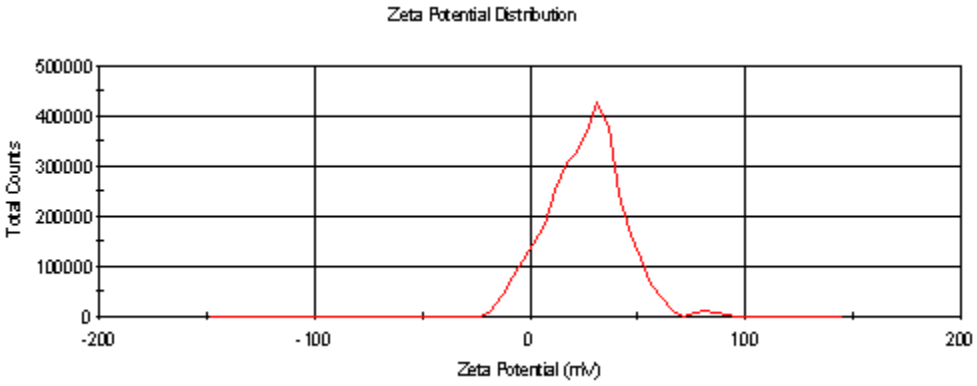

Fig. 6.5(B) *Zeta potential plot of ZnS-CdS core-shell nanoparticles.*

It can be seen in both the core shell models the zeta potential is slightly positive (around 40*m*V). In spite of having a non polar solvent the zeta potential is positive. Particles on the surface will repel each other. This will resist aggregation and confer stability of the solution. Thus zeta potential can also be used to increase the shelf life of the nanoparticles.

6.6 Summary

- Mixed nanoparticles consisting of two semiconductors can be heterogeneously connected (Composite nanoparticles). They are coated particles with Core- Shell structure. Mixed semiconductor system offers potential advantages for solar energy utilization because of the possibilities presented by inter-particle electron transfer and special properties.
- CdS – ZnS / ZnS – CdS Core- shell nanoparticles of a controlled diameter can be synthesized at room temperature in organic phase. It is seen that the shell does not coagulate with the core particles.
- UV- vis absorption spectra are consistent with narrow size distribution and excellent particle quality.
- The study of particle size analysis reflects the average size of the nanoparticles synthesized ranging around 100nm.

6.7 References

[1] Audinet, L.; Ricolleau, C.; Gandais, M.; Gacoin, T.; Boilot, J. P.; Buffat, P. A. *Philosophical Mag. A,* **1999**, *Vol 79 (10), 2379* .

[2] Cao, Y. W.; Banin, U. *Angew. Chem . Int. Ed.*, **1999**, *38, 3692.*

[3] Chen, .X; Nazzal, A.; Goorskey, D.; Xiao, M.; Peng, Z. A.; Peng, X. *Phys. Rev. B,* **2002**, *64, 245304.*

[4] Harrison, M. T.; Kershaw, S. V.; Rogach, A. L.; Kornowski, A.; Eychmuller, A.; Weller, H. *Adv. Mater.*, **2000**, *12, 123.*

[5] Taleb Mokari, Uri Banin *Chem. Mater*. **2003**, *15,3955.*

[6] Colvin, V. L.; Schlamp, M. C.; Alivistos, A. P. *Nature,* **1994**, *370, 354.*

[7] Dabhousi, B. O.; Onitsuka, O.; Bawendi, M. G.; Rubner, M. F. *Appl. Phys. Lett.*, **1995**, *66, 1316.*

[8] Bruchez, Jr., M.; Moronne, M.; Gin, P.; Weiss, S.; Alivisatos, P. A. *Science,* **1998**, *281, 2013.*

[9] Chan, W. C. W.; Nie, S. *Science,* **1998**, *281, 2016.*

[10] Mattoussi, H.; Mauro, I. M.; Goldman, E. R.; Anderson, G. P.; Sundar, V. C.; Mikulec, F. V.; Bawendi, M. G. *J. Am. Chem. Soc.*, **2000**, *122, 12142.*

[11] Coe, S.; Woo, W. K.; Bavendi, M.; Bulovic, V. *Nature,* **2002**, *420, 800.*

[12] Tessler, N.; Medvedev, V.; Kazes, M.; Kan, S. H.; Banin, U. *Science,* **2002**, *295, 1506.*

[13] Steckel, J. S.; Coe-Sullivan, S.; Bulovic, V.; Bavendi, M. G. *Adv. Mater,* **2003**, *15, 1862.*

[14] Allais, M.; Gandais, M. *Phil Mag. Lett.,* **1992**, 65, 243.

[15] Herron, N.; Wang, Y.; Eddy, M. M.; Stucky, G. D.; Cox, D. E.; Moller, K.; Bein, T. *J. Am. Chem. Soc.,* **1989**, 111, 530

[16] Zhao, X. K.; Yang, J.; Mc-Cormick, L. D.; Fendler, J. H. *J. Phys. Chem.*, **1992**, 96, 9933

[17] Murry, C.B.; Norris, D.J.; Bawendi, M.G. *J. Am. Chem. Soc.*, **1993**, *115, 8706.*

[18] Pileni, M.P. *Adv. Colloid Interface Sc.*, **1993**, *46, 139.*

[19] Peng, X.G.; Wicham, J.; Alivisatos, A.P. *J. Am. Chem. Soc.* **1998**, 120, 5343